Morphology and Performance of Polyvinylidene Fluoride/Perfluorosulphonic Acid Hollow Fibre Ultrafiltration Blend Membranes

Guo-Lin Yuan[1,2], Zhen-Liang Xu[1,2*], Yong-Ming Wei[2], and Li-Yun Yu[2]

(1) State Key Laboratory of Chemical Engineering, East China University of Science and Technology, PR China
(2) Membrane Science and Engineering R&D Lab, Chemical Engineering Research Center, ECUST, Shanghai 200237, PR China

A B S T R A C T

Polyvinylidene fluoride (PVDF)-perfluorosulphonic acid (PFSA) hollow fibre ultrafiltration (UF) blend membranes were prepared by wet-spinning method. Polyvinylpyrrolidone (PVP) and ethanol aqueous solutions were employed as additive and coagulants, respectively. The effect of PVP concentration in the dopes and ethanol concentration in the coagulants on morphology and performance of PVDF-PFSA hollow fibre UF blend membranes were investigated. Blend membranes were characterized in terms of precipitation kinetics, morphology, thermal property and separation performance. The results showed that the increments of PVP concentration in the dopes and ethanol concentration in coagulants both resulted in higher pure water permeation flux (PWP) and worse rejection (R) of bovine serum albumin (with the increment of PVP concentration from 0 to 5 wt% in the dopes, PWP increased from 41.7 L.m^{-2}.h^{-1} to 134 L.m^{-2}.h^{-1} and R decreased from 99.8% to 84.4% as well as with the increase in ethanol concentration in coagulants from 0 to 40 wt%, PWP increased from 33.5 L.m^{-2}.h^{-1} to 123 L.m^{-2}.h^{-1} and R decreased from 97.7% to 88.7%). However, the proportion of sponge-like structure in the cross-section of membranes decreased with the increasing PVP concentration in the dopes and the proportion increased with the increased ethanol concentration in the coagulations. In addition, the location of the sponge-like structure in the cross-section of membranes was significantly influenced by ethanol concentrations in the coagulants and DSC results revealed that the crystallinity (X_c) of the blend membrane was in accordance with the proportion of sponge-like structure. These behaviours were attributed to the different roles of PVP in the dopes and ethanol in the coagulants, respectively. PVDF-PFSA hollow fibre membranes with different morphologies and performances were prepared by these two different routes. Meanwhile, the range of PVDF-PFSA hollow fibre blend membranes was extended.

INTRODUCTION

Polyvinylidene fluoride (PVDF) possesses excellent thermal properties and perfect chemical resistance to the corrosive chemicals and organic compounds. As a semi-crystalline polymer, due to its more complicated phase separation phenomenon compared with the amorphous polymers [1], it has received increasing attention in the field of membrane separation applications. During the non-solvent induced phase separation (NIPS) process, the effect of polymer concentration, solvent/non-solvent system, additives and blend polymers in the dopes have been described and emphasized [2-5].

(∗) To whom correspondence to be addressed.
E-mail: chemxuzl@ecust.edu.cn

The introduction of non-solvent additives in the PVDF dopes is an effective way to increase the precipitation rate [6]. Shi et al. [7] and Wang et al. [8] investigated the effects of PEG and PVP on morphology of PVDF membranes, respectively. The effect of PVP on the phase inversion behaviour of PVDF/DMAc/water ternary system was reported by Yeow et al. [9]. Some investigations were carried out to prepare various blend membranes, such as porous polyvinylidene fluoride-thermoplastic polyurethane (PVDF-TPU) blend hollow fibre membranes [10,11], polyvinylidene fluoride-*co*-hexafluoropropylene (PVDF-HFP) microporous hollow fibre membranes [7] and others as well [12].

Different morphologies of PVDF membranes could be obtained with different spinning conditions such as extrusion rate, air gap and coagulant [7,16-21] and different dopes [11-15]. From the viewpoint of environmental protection, the ethanol/water system is widely used as a coagulant to prepare the membranes with different morphologies [22]. The inner skin layer of hollow fibre changes to a loose porous network with ethanol as an internal coagulant [8]. Kong et al. [6] found that external skin layer could be completely eliminated with 50% (v/v) ethanol aqueous solution as external coagulant, and similarly the inner skin layer could also be completely removed with anhydrous ethanol as the internal coagulant. However, for a PVDF/DMAc/PVP/LiCl dope, a solution of 50 wt% ethanol could not lead to skinless surface [23].

Perfluorosulphonic acid (PFSA) actually exhibits a good miscibility with PVDF [24]. The PVDF-PFSA blend membranes have been used in the chlor-alkali industry and ion-exchange membrane in fuel cell [25,26]. Lang et al. [27] have prepared PVDF-PFSA hollow fibre UF blend membranes. The addition of non-solvent additives in dope solution would be a good way to improve the performance of the PVDF-PFSA membranes and meanwhile the different water/ethanol fabricating coagulations may extend the range of PVDF-PSFA membranes. To the best of our knowledge, the effects of PVP in dope solution and composition of coagulations on PVDF-PFSA hollow fibre have not been reported. This present investigation aimed to prepare PVDF-PFSA hollow fibre blend membranes with different morphologies

and performances by introducing PVP in the dopes and ethanol in the coagulant. Thus, the effects of PVP concentration in dopes and ethanol concentrations in the internal and external coagulants were systematically studied on the morphologies and properties of PVDF-PFSA blend membranes by precipitation kinetics, thermal properties and separation performances.

EXPERIMENTAL

Materials
PVDF (FR904) powder was purchased from Shanghai San Ai Fu Co. Ltd. (China), and PFSA granules from Shanghai Bai-Chun Chemical Materials Co. Ltd. (China). *N,N*-Dimethylacetamide (DMAc) and glycerol were from Shanghai Jing-Wei Chemical Reagent Co. Ltd. (China), as well as ethanol, PEG (M_w = 400), PVP (K30) and bovine serum albumin (BSA) from Shanghai Sinopharm Chemical Reagent Co. Ltd. (China).

Preparation of the Blend Membranes
The spinning dopes were prepared by mixing PVDF, PFSA, PEG, PVP and DMAc under continuous agitation. After forming homogeneous solutions, the spinning dopes were degassed at 50°C. The composition of the solution was 19 wt% PVDF, 1 wt% PFSA and 5 wt% PEG with the remainder comprising
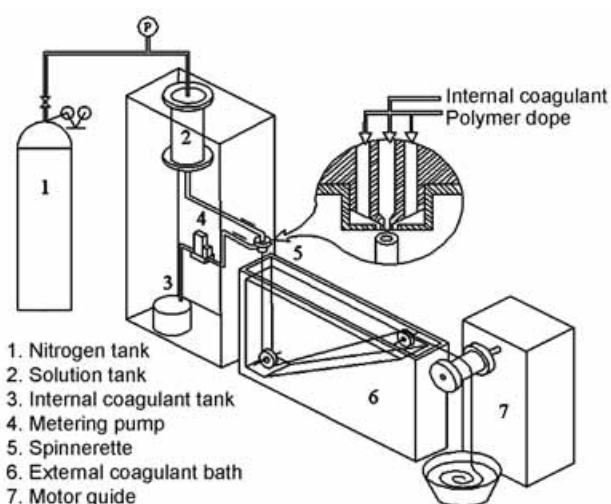

Figure 1. Scheme of PVDF-PFSA hollow fibre preparation setup.

Table 1. Concentrations of PVP in the dopes and ethanol in coagulants for different hollow fibre membranes.

Membrane	PVP concentration in the dope (wt%)	Ethanol concentration (wt%)	
		External coagulation	Internal coagulation
M-0PVP	0	50	50
M-1PVP	1	50	50
M-3PVP	3	50	50
M-5PVP	5	50	50
M-5000	5	50	0
M-5010	5	50	10
M-5020	5	50	20
M-5030	5	50	30
M-5040	5	50	40
M-0050	5	0	50
M-1050	5	10	50
M-2050	5	20	50
M-3050	5	30	50
M-4050	5	40	50

PVP and DMAc. Aqueous ethanol solutions (0 to 50 wt%) were used as internal and external coagulants, respectively at room temperature (25ºC). The dopes were kept at 50°C, and the hollow fibre blend membranes were spun by wet-spinning method (the air gap was 0 cm) which was described in previous report [27] using the spinning apparatus (Figure 1). Nascent hollow fibres were collected by a roller at a free falling velocity. Then, the membranes were stored in a deionized water bath to remove resid-ual solvent; followed by keeping in 50 wt% glycerol aqueous solution. The concentrations of PVP used in the dopes and concentrations of ethanol used in the internal and external coagulants for different PVDF-PFSA hollow fibre membranes are listed in Table 1.

Light Transmittance Measurement

Analysis of light transmittance curves is a simple method to investigate the coagulation kinetics [28]. The curves have been obtained by immersing dopes in non-solvent baths, with a self-made device [29,30]. Taking, for example, a beam of laser passed through a dope-cast plate that was immersed in a coagulation bath and an optical detector detecting the transmitted light intensity to produce signals which were consequently converted, amplified and then recorded by a computer. The precipitation rate of the dope

solution was investigated by the curve of transmitted light intensity versus immersion time.

Calculations of Solubility Parameters

Solubility parameters could be used to describe interactions qualitatively between polymer and non-solvent and solvent and non-solvent [28]. Based on the solubility parameters and molecular volume in Table 2 [31], the solubility parameters of the various coagulations (δ) were calculated by eqn (1) and the differences of solubility parameters between the coagulants and solvent and the coagulants and polymer were calculated by eqn (2) [28]:

$$\delta_i = \frac{X_1 V_1 \delta_{i,1} + X_2 V_2 \delta_{i,2}}{X_1 V_1 + X_2 V_2}, i = d, p, h \tag{1}$$

$$\Delta\delta_{j-n} = [(\delta_{d,j} - \delta_{d,n})^2 + (\delta_{p,j} - \delta_{p,n})^2 + (\delta_{h,j} - \delta_{h,n})^2]^{1/2} \tag{2}$$

where δ is the solubility parameter, X is the molecular fraction and V is the molecular volume. Subscripts 1 and 2, in eqn (1), stand for water and ethanol, respectively. Subscripts d, p and h stand for the dispersive, polar and hydrogen-bonding

Table 2. Solubility parameter and molecular volume of DMAc, ethanol and water [31].

Substance	δ_d (MPa)$^{1/2}$	δ_p (MPa)$^{1/2}$	δ_h (MPa)$^{1/2}$	δ (MPa)$^{1/2}$	v (cm^3/mol)
PVDF	17.2	12.5	9.2	23.2	-
DMAc	16.8	11.5	10.2	22.7	92.5
Water	15.5	16.0	42.4	47.9	18.0
Ethanol	15.8	8.8	19.4	26.6	58.5

components of the solubility parameter, respectively. The notation n stands for coagulant and j stands for solvent or polymer.

The results are listed in Table 3. δ_{s-n} is the difference of solubility parameter between solvent and coagulation. δ_{p-n} is the difference of solubility parameter between polymer and coagulation.

Characterization of Membrane Morphology

The morphology of the membranes was inspected by scanning electron microscopy (SEM) (Jeol Model JSM-6360 LV, Japan). The wet membranes taken from the glycerol/water solution were firstly immersed in ethanol for 12 h, then immersed in hexane for 12 h and finally dried in air. The treated membranes were frozen in liquid nitrogen for a few minutes and carefully fractured. These samples were deposited on a copper holder, coated with sputtering gold under vacuum and then transferred under the microscope for imaging.

The proportion of finger-like voids area in the whole cross-section (P_f) was calculated by eqn (3):

$$P_f = \frac{S_f}{S_m} \times 100\% \qquad (3)$$

Table 3. Calculated values of δ, δ_{s-n} and δ_{p-n}.

Substance	δ (MPa)$^{1/2}$	δ_{s-n} (MPa)$^{1/2}$	δ_{p-n} (MPa)$^{1/2}$
Water	-	31.3	33.4
Ethanol:			
10 wt%	45.3	29.6	22.5
20 wt%	42.8	26.8	20.0
30 wt%	40.4	24.2	17.6
40 wt%	38.1	21.7	15.4
50 wt%	36.0	19.4	13.5

where S_f is the area of finger-like voids in the cross-section of membrane (mm^2) (near inner layer for M-5000, M-5010, M-5020, M-5030 and M-5040; near outer layer for M-0050, M-1050, M-2050, M-3050 and M-4050), S_m is the whole cross-sectional area of the hollow fibre membrane (mm^2). S_f and S_m were obtained with software located on the cross-sections of the membrane in SEM photographs.

DSC Analysis

The crystallinity (X_c) of PVDF crystals in various membranes was determined by means of thermal analysis. The differential scanning calorimeter (DSC) (Diamond, Perkin Elmer, USA) was used to measure the thermal properties of the membranes. The samples of membranes were heated under nitrogen atmosphere at a rate of 10ºC/min in all the experiments. The melting temperature (T_m) and heat of fusion (ΔH_m) data of different membranes were obtained as a mean average value of 3 tests on each sample. The X_c for each membrane was calculated based on the heat of fusion data of ideal PVDF crystal ($\Delta H_m^0 = 105$ mJ/mg) [32].

Separation Performance Test

All the tests were performed at room temperature with a constant pressure of 0.1 MPa and the BSA concentration of the feed solution was 500 ppm. The concentrations of permeate and feed solutions were determined by UV-spectrophotometry (Shimadzu UV-3000, Japan). The pure water permeation flux (PWP) and rejection (R) of BSA were defined as eqns (4) and (5) [29]. The experimental data were measured 3 times for each kind of membrane and then averaged.

$$PWP = \frac{Q}{t \times A} \qquad (4)$$

$$R = \left(1 - \frac{C_P}{C_F}\right) \times 100\% \qquad (5)$$

where PWP is the pure water permeation flux (L.m^{-2}.h^{-1}), Q is the volume of permeate pure water (L), A is the effective area of the hollow fibre membrane in the modules (m^2) and t is the permeate time (h). R is the rejection of the BSA, C_P and C_F are the BSA concentrations (wt%) in permeate and feed solutions respectively.

RESULTS AND DISCUSSION

Effect of Dope PVP Concentration and Coagulant Ethanol Concentration on NIPS Process

Figure 2 shows the light transmittance curves characterized by immersing the dopes with different PVP concentrations into 50 wt% ethanol coagulation bath. According to the studies by Reuvers et al. [33,34], the precipitation process can be divided into instantaneous demixing and delayed demixing under different delayed times. In Figure 2, the phase inversion is all shown to be slow and tend to delay demixing for different dopes immersed in 50 wt% aqueous ethanol solution.

The transmitted light intensity is decreased with time except an increase at the start for the dopes containing PVP, which is in accordance with the
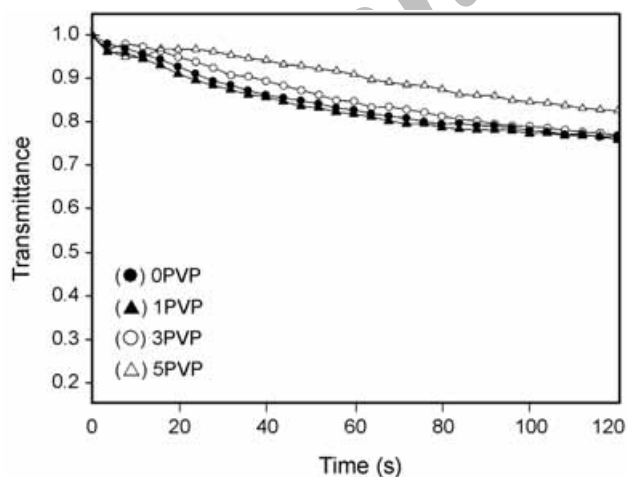
report of Yang et al. [35]. The skin is formed faster due to PVP in the dope, and consequently limit the DMAc diffusion out of the nascent membrane. Therefore, a high local concentration of solvent was formed which could result in partial dissolution of precipitated PVDF. Further investigations are being carried out for more in-depth studies on this phenomenon.

Figure 3 illustrates the light transmittance changes with the increase in ethanol concentration for the dopes with 5 wt% PVP. The light transmittance has declined immediately and sharply after immersing the dope in contact with water (0 wt% ethanol) and the precipitation rate has also decreased with increasing ethanol concentration in the coagulation from 10 wt% to 50 wt%. The redissolution of PVDF has also occurred in these precipitation processes, thus the transmittance curves of 30 wt%, 40 wt% and 50 wt% ethanol are crossed each other.

The precipitation rate of polymer dope was determined by the thermodynamics and kinetics of the process. Both δ_{s-n} and δ_{p-n} decreased with increasing concentration of ethanol in coagulation (Table 3). The mixing of solvent and coagulant is easier and the precipitation is faster when δ_{s-n} is smaller. On the other hand, smaller δ_{p-n} implies that more coagulant might be needed for NIPS process. Meanwhile, according to the diffusion coefficients of non-solvent and solvent (Table 4 [23,36]), $D_{DMAc-in-water}$ and
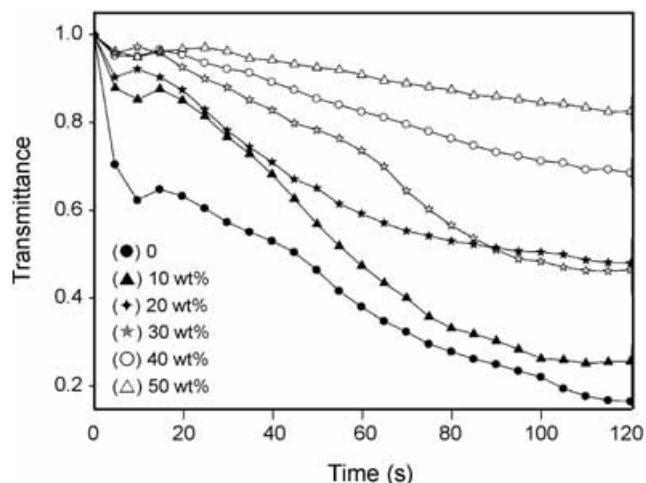
Figure 2. Light transmittance curves obtained by immersing the dopes containing different PVP (0, 1, 3 and 5 wt%) into 50 wt% ethanol aqueous solution.

Figure 3. Light transmittance curves obtained by immersing dopes containing 5 wt% PVP into coagulation with different ethanol concentrations: 0, 10, 20, 30, 40 and 50 wt%.

Table 4. Diffusion coefficient of non-solvent and solvent [22,36].

Diffusion coefficient	$D \times 10^5$ (cm²/s)
$D_{DMAc-in-water}$	0.91
$D_{DMAc-in-ethanol}$	1.08
$D_{Water-in-DMAc}$	1.68
$D_{Ethanol-in-DMAc}$	0.04

$D_{DMAc-in-ethanol}$ are similar, and the diffusion rate of ethanol in DMAc is smaller than that of water in DMAc. Thus, more ethanol in the coagulation has led to slower diffusion of coagulant into the dope. The final precipitation rate of the dope is dependent on the comprehensive result of the above two effects. Figure 3 confirms that more ethanol in coagulation decreased the precipitation rate of this dope system.

Effect of Dope PVP Concentration and Coagulant Ethanol Concentration on the Morphology of PVDF-PFSA Hollow Fibre UF Blend Membranes

Figure 4 displays the cross-section morphologies of the PVDF-PFSA membranes. Finger-like voids and cavities are absent in the whole cross-section of the hollow fibre without PVP in dope (M-0PVP). Cavities have appeared near the inner layer, for the dope with 1 wt% PVP (M-1PVP) and near both inner and outer layers for the dope with 3 wt% PVP (M-3PVP). With the increasing PVP concentration, the number of cavities increased (M-5PVP). Although the sponge-like structures occupied most of the cross-section, the finger-like voids and cavities gradually increased with the addition of PVP, which suggested PVP in the dopes could promote the formation of finger-like pores and cavities in the fibre cross-section. Shi et al.
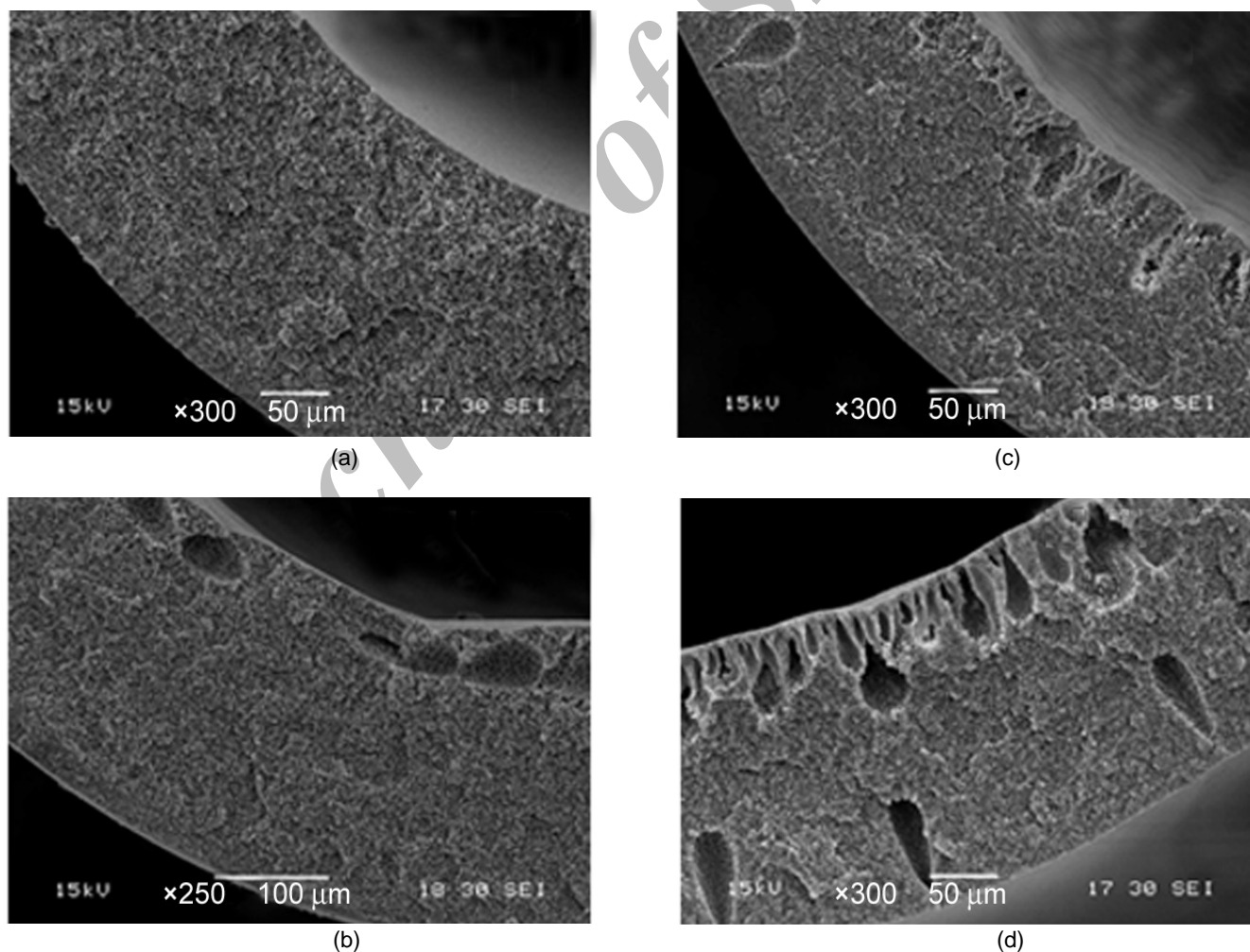

(a)   (c)

(b)   (d)

Figure 4. SEM photographs for cross-section of hollow fibres with different PVP concentrations: (a) without PVP (M-0PVP), (b) with 1 wt% PVP (M-1PVP), (c) 3 wt% PVP (M-3PVP), and (d) 5 wt% PVP (M-5PVP).
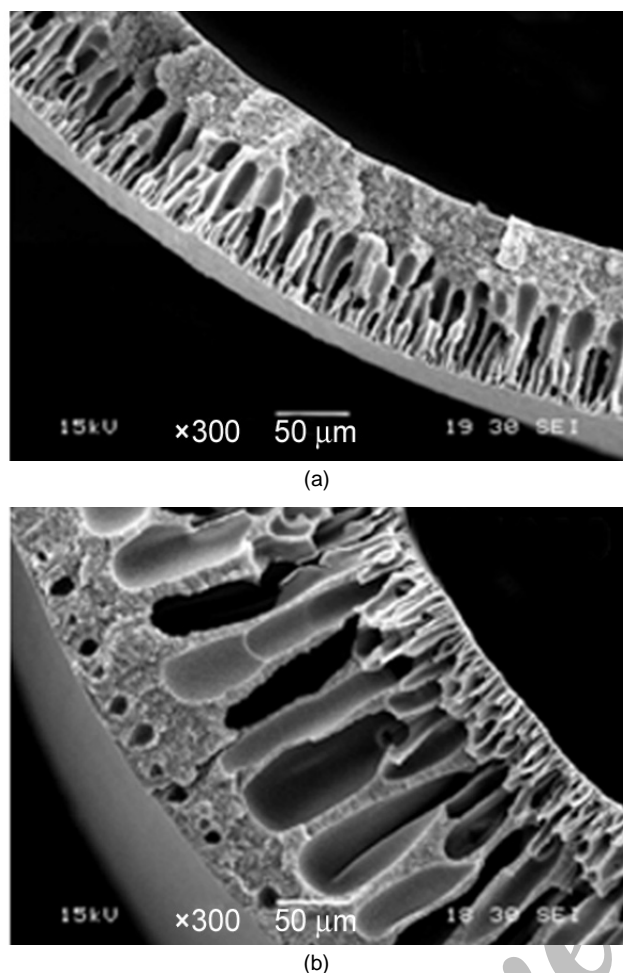
(a)

(b)

Figure 5. SEM photographs for surfaces and cross-section of membranes: (a) M-0050 and (b) M-5000.

[7], also found that up to 5 wt% PVP in the dope favoured the development of the macrovoid in PVDF membranes.

Figure 5 shows the morphologies of membranes M-5000 and M-0050. The effect of ethanol concentration of internal coagulation on the morphologies of membranes is presented in Figure 6. As shown in Figure 5 (M-5000) and Figure 6, the finger-like voids under the inner layer diminished with increasing

ethanol concentration in the internal coagulant. In Table 5, P_f of M-5000 is 69.7%; P_f of M-5010, M-5020, M-5030 and M-5040 are decreased from 60.0% to 36.8% when the ethanol concentration is increased from 10 wt% to 40 wt% in the internal coagulant. Smaller cavities near the outer surface (generated in 50 wt% ethanol aqueous solution) are remained almost unchanged. The sponge-like structure is relatively thicker. It is reported that pure ethanol using as internal coagulant makes finger-like voids disappear for PVDF membranes spun from the dope consisting 5 wt% PVP by Wang et al. [8]

Figure 7 illustrates the effect of ethanol concentration in the external coagulation on morphologies of membranes. As it is observed, the finger-like structure is decreased with the incremental increase of ethanol concentration in external coagulation. P_f of M-1050, M-2050, M-3050 and M-4050 decreased from 52.2% to 23.1% with increasing ethanol concentration in external coagulant from 10 wt% to 40 wt% (Table 5). This confirms that the increased ethanol concentration in the coagulation bath has led to a shift in the membrane morphology from finger-like voids to sponge-like structures. PVDF hollow fibre membranes without finger-like voids near the outer layer could be spun from a dope without PVP additive and coagulated in 50% (v/v) aqueous ethanol solution used as external coagulant [22] as well as M-0PVP. The morphology of M-0050 is shown in Figure 5. There are no small cavities near inner layer of M-0050. The reason for this phenomenon is under further investigation.

Comparing with the morphologies of PVDF-PFSA hollow fibre blend membranes in Figures 6 and 7, the locations of sponge-like structures depend on the relative coagulating power of the internal and external coagulants, e.g., for M-5010 the sponge-like structure is formed near the outer layer but for M-

Table 5. Proportion of finger-like voids area in cross-section of different membranes.

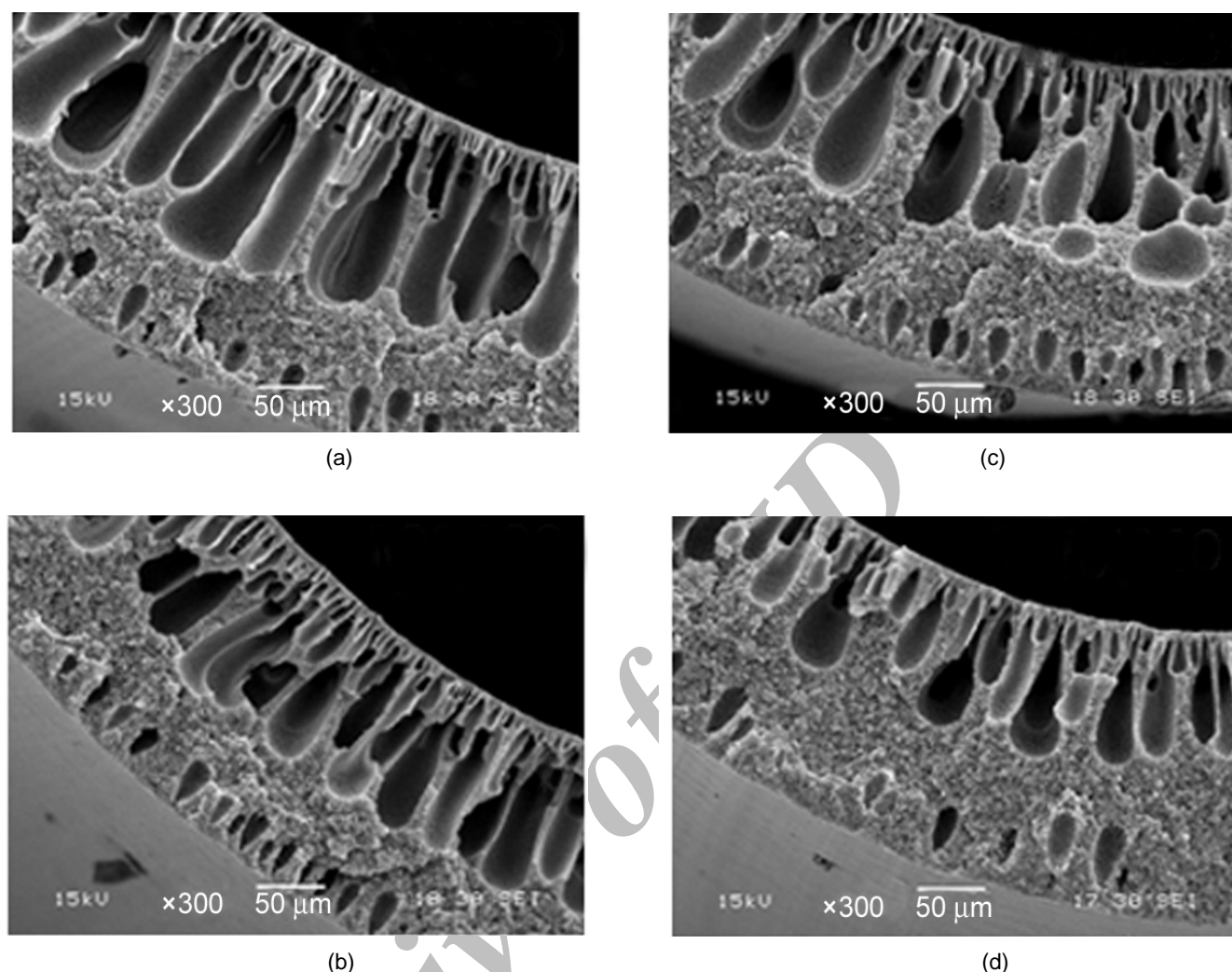| Membrane	P_f near inner layer (%)	Membrane	P_f near outer layer (%)
M-5000	69.7	M-0050	54.6
M-5010	60.0	M-1050	52.2
M-5020	51.3	M-2050	45.0
M-5030	44.7	M-3050	37.5
M-5040	36.8	M-4050	23.1

(a)

(c)

(b)

(d)

Figure 6. Effect of ethanol concentrations ((a) 10 wt% (M-5010), (b) 20 wt% (M-5020), (c) 30 wt% (M-5030), and (d) 40 wt% (M-5040)) as internal coagulant on the morphology of membrane when 50 wt% concentration of aqueous ethanol solution is as the external coagulant.

1050 the location of the sponge-like structure is near the inner layer.

In Figures 5-7, the presence of the inner and outer skin layers may be observed which indicates that 50 wt% aqueous ethanol solution as internal and/or external coagulants could not form the inner and/or external skinless surface of PVDF-PFSA hollow fibre membranes for this dope system. This is different from the morphologies of membrane prepared by Kong et al. [6]. For PVDF/PVP/DMAc dope system, using 50% (v/v) of aqueous ethanol solution as the external coagulation bath there would be a total elimination of the external skin layer. In the present work, the PFSA in dopes has the sulphonic group side chains which have strong binding capacity with water

and ethanol molecules [37]. Hence, it enhances the diffusion of coagulant and favours the formation of skin layer during the precipitation process.

Thermal Properties of PVDF-PFSA Hollow Fibre UF Blend Membranes

The results of T_m, ΔH_m and X_c, obtained by means of DSC thermal analysis, are summarized in Table 6. All the membranes have exhibited a similar melting behaviour with a broad melting peak around 162°C. As the concentration of PVP is increased from 0 to 5 wt%, X_c is dramatically decreased from 52.6% to 44.0%. This is in accordance with the fact that less structural areas of the membrane have sponge-like morphology. X_c of membranes prepared from the
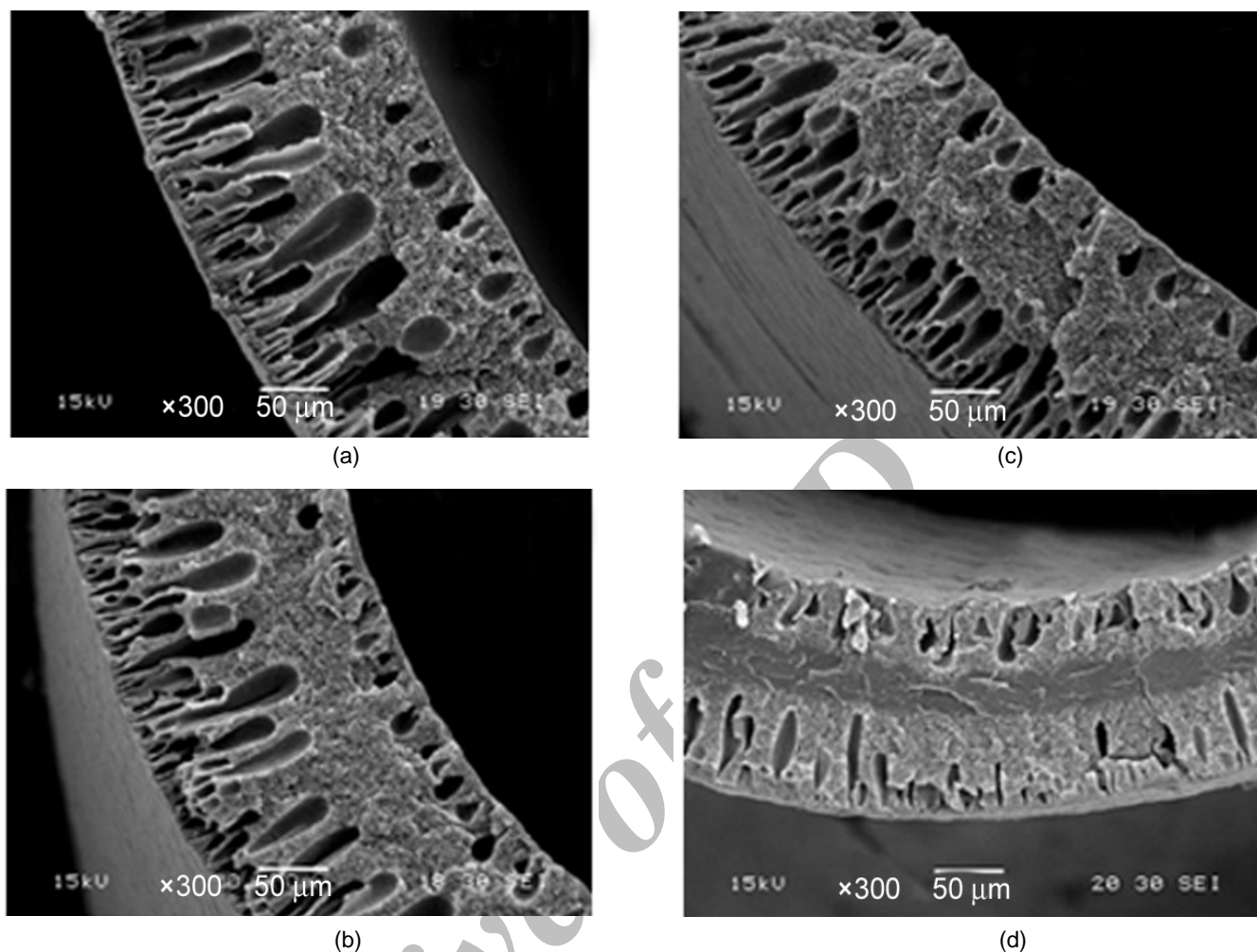
(a)

(c)

(b)

(d)

Figure 7. Effect of ethanol concentrations ((a) 10 wt% (M-1050), (b) 20 wt% (M-2050), (c) 30 wt% (M-3050), and (d) 40 wt% (M-4050)) as external coagulant on the morphology of membrane when 50 wt% concentration of aqueous ethanol solution is as the internal coagulant.

same dope is slightly increased when more ethanol has been introduced in coagulants. X_c has been maximized at 44.0% when the ethanol concentrations of internal and external coagulants were both 50 wt%. The liquid-liquid demixing taking place before the nucleation process of crystallization leads to finger-like voids. In contrast, if the mass transfer is slow enough, crystallization occurs prior to the liquid-liquid dimixing and thus sponge-like structure is formed [38]. PVDF plate membranes with higher crystallinity were prepared before with immersion precipitation method in 1-octanol by Young et al. [38].

Separation Performance of PVDF-PFSA Hollow Fibre UF Blend Membranes

For PVDF-PFSA hollow fibre blend membranes,

when entrapped by membrane materials PVP improves the permeate flux (Table 6), since it increases the hydrophilicity of the membranes [39]. The water flux of membranes is increased when PVP is bleached out as additive [10]. Growth of polymer crystallinity has a detrimental effect on the final membrane permeation properties [40]. Without PVP, PVDF hollow fibre membrane has low permeate fluxes (41.7 $L.m^{-2}.h^{-1}$). When PVP in PVDF-PFSA dopes is increased from 1 wt% to 5 wt%, the crystallinity is reduced, PWP is enhanced from 61.2 $L.m^{-2}.h^{-1}$ to 134 $L.m^{-2}.h^{-1}$ and R is simultaneously decreased from 98.9% to 84.4% in Table 6. Yuan et al. [10] and Shi et al. [7] have also reported that PVP-K30 for PVDF-TPU and PVDF-PHF blend membranes operate as a permeate flux enhancer,

Table 6. Thermal and separation properties of different PVDF-PFSA membranes.

Membrane	T_m (°C)	ΔH_m (mJ/mg)	X_c (%)	PWP (L.m^{-2}.h^{-1})	R (%)
M-0PVP	163.2 ± 0.1	55.2 ± 0.2	52.6 ± 0.1	41.7 ± 3.0	99.8 ± 0
M-1PVP	162.9 ± 0.2	52.7 ± 0.6	50.3 ± 0.3	61.2 ± 2.7	98.9 ± 0.2
M-3PVP	162.5 ± 0.2	48.5 ± 0.5	46.3 ± 0.2	108 ± 5.0	92.8 ± 1.0
M-5PVP	162.2 ± 0.1	46.2 ± 0.7	44.0 ± 0.3	134 ± 4.8	84.4 ± 1.2
M-5000	161.2 ± 0.2	41.8 ± 0.4	39.9 ± 0.2	33.5 ± 2.0	95.4 ± 0.9
M-5010	161.8 ± 0.3	43.1 ± 0.1	41.0 ± 0	42.8 ± 5.5	95.2 ± 0.3
M-5020	162.2 ± 0.2	43.6 ± 0.1	41.5 ± 0	97.2 ± 3.0	94.6 ± 0.5
M-5030	162.2 ± 0.1	43.4 ± 0.2	41.4 ± 0	98.1 ± 2.1	94.1 ± 0.7
M-5040	161.8 ± 0.2	44.6 ± 1.4	42.5 ± 0.3	123 ± 6.9	93.2 ± 1.6
M-0050	161.9 ± 0.3	43.5 ± 0.3	41.4 ± 0.1	35.5 ± 5.0	97.7 ± 2.0
M-1050	161.5 ± 0.3	44.0 ± 0.3	41.9 ± 0.1	41.9 ± 6.3	95.6 ± 0.8
M-2050	161.9 ± 0.2	44.2 ± 0.1	42.1 ± 0	68.6 ± 2.0	94.7 ± 0.4
M-3050	162.2 ± 0.0	44.6 ± 0.3	42.5 ± 0.1	113 ± 7.7	94.4 ± 0.7
M-4050	162.2 ± 0.1	45.1 ± 0.4	43.0 ± 0.2	116 ± 6.0	88.7 ± 1.1

respectively. Besides, with the incremental increase of ethanol concentration from 0 to 50 wt% in internal coagulation, PWP is increased from 33.5 L.m^{-2}.h^{-1} to 123 L.m^{-2}.h^{-1} and R of BSA is decreased from 95.4% to 93.2%, respectively. When ethanol concentration of external coagulation is increased from 0 to 50 wt%, PWP is also enhanced from 35.5 L.m^{-2}.h^{-1} to 116 L.m^{-2}.h^{-1} and R is decreased from 97.7% to 88.7%, respectively. The results from the UF experiments reveal that the PVDF-PFSA hollow fibre UF blend membranes with different permeation performances could be prepared when ethanol concentration is variable in internal/external coagulants.

CONCLUSION

A series of PVDF-PFSA hollow fibre UF blend membranes with different morphologies and performances were successfully prepared by wet-spinning method. Effects of ethanol concentrations in the internal and external coagulants and PVP concentration in the dopes on inversion process, morphology, thermal properties and separation performances of the PVDF-PSA hollow fibre membranes were studied. It was found that the sponge-like structures possess the whole cross-section of the membrane without PVP in

the dope. With the increase of PVP concentration from 1 wt% to 5 wt% in dopes, macrovoid in cross-section is gradually increased. As the ethanol concentrations in internal or external coagulants are increased from 0 to 50 wt%, the proportions of long finger-like voids near inner layer or outer layer are gradually decreased. The proportion and location of the sponge-like structures depend on ethanol concentrations in the internal and external coagulants. 50 wt% aqueous ethanol solution using as internal or/and external coagulants could not eliminate inner and/or external skin layers of PVDF-PFSA hollow fibre membranes. PWP has been enhanced and R is decreased as PVP concentration in the dope and ethanol concentration in the coagulant are increased, respectively. The results of thermal property from DSC examination revealed that the crystallinity (X_c) of the blend membrane is in accordance to the proportion of sponge-like morphologies.

REFERENCES

1. Cao JH, Zhu BK, Xu YY, Structure and ionic conductivity of porous polymer electrolytes based on PVDF-HFP copolymer membranes, *J Membr Sci*, **281**, 446-453, 2006.

2. Khayet M, Feng CY, Khulbe KC, Matsuura T, Study on the effect of a non-solvent additive on the morphology and performance of ultrafiltration hollow-fiber membranes, *Desalination*, **148**, 321-327, 2002.

3. Yeow ML, Isothermal phase diagrams and phase-inversion behavior of poly(vinylidene fluoride)/solvents/additives/water systems, *J Appl Polym Sci*, **90**, 2150-2155, 2003.

4. Quirin JC, Torkelson JM, Self-referencing fluorescence sensor for monitoring conversion of nonisothermal polymerization and nanoscale mixing of resin components, *Polymer*, **44**, 423-432, 2003.

5. Shi L, Wang R, Cao YM, Liang DT, Tay JH, Effect of additives on the fabrication of poly(vinylidene fluoride-*co*-hexafluropropylene) (PVDF-HFP) asymmetric microporous hollow fiber membranes, *J Membr Sci*, **315**, 195-204, 2008.

6. Kong JF, Li K, Preparation of PVDF hollow-fiber membranes via immersion precipitation, *J Appl Polym Sci*, **81**, 1643-1653, 2001.

7. Shi L, Wang R, Cao YM, Feng CH, Liang DT, Tay JH, Fabrication of poly(vinylidene fluoride-*co*-hexafluropropylene) (PVDF-HFP) asymmetric microporous hollow fiber membranes, *J Membr Sci*, **305**, 215-225, 2007.

8. Wang DL, Li K, Teo WK, Preparation and characterization of polyvinylidene fluoride (PVDF) hollow fiber membranes, *J Membr Sci*, **163**, 211-220, 1999.

9. Yeow ML, Liu YT, Li K, Isothermal phase diagrams and phase-inversion behavior of poly(vinylidene fluoride)/solvents/additives/water systems, *J Appl Polym Sci*, **90**, 2150-2155, 2003.

10. Yuan Z, Xi DL, Porous PVDF/TPU blends asymmetric hollow fiber membranes prepared with the use of hydrophilic additive PVP (K30), *Desalination*, **223**, 438-447, 2008.

11. Zhou Y, Xi DL, Effect of PVP additive on PVDF/TPU blend hollow fiber membranes by phase inversion, *Iran Polym J*, **16**, 241-250, 2007.

12. Lin F, Li Q, Jiang DB, Yu XH, Li L, Thermoresponsive microfiltration membranes prepared by atom transfer radical polymerization directly from poly(vinylidene fluoride), *Iran Polym J*, **18**, 561-568, 2009.

13. Yu LY, Xu ZL, Shen HM, Yang H, Preparation and characterization of PVDF-SiO₂ composite hollow fiber UF membrane by sol-gel method, *J Membr Sci*, **337**, 257-265, 2009.

14. Yu LY, Shen HM, Xu ZL, PVDF-TiO₂ composite hollow fiber UF membranes prepared by TiO₂ sol-gel method and blending method, *J Appl Polym Sci*, **113**, 1763-1772, 2009.

15. Xu ZL, Yu LY, Han LF, Polymer-nanoinorganic particles composite membranes: a brief overview, *Front Chem Eng China*, 2009, DOI: 10.1007/s11709-009-0199-7.

16. Albrecht W, Kneifel K, Weigel T, Hilke R, Just R, Schossig M, Ebert K, Lendlein A, Preparation of highly asymmetric hollow fiber membranes from poly(ether imide) by a modified dry-wet phase inversion technique using a triple spinneret, *J Membr Sci*, **262**, 69-80, 2005.

17. Wang KY, Matsuura T, Chung TS, Guo WF, The effects of flow angle and shear rate within the spinneret on the separation performance of poly(ethersulfone) (PES) ultrafiltration hollow fiber membranes, *J Membr Sci*, **240**, 67-79, 2004.

18. Shen LQ, Xu ZK, Liu ZM, Xu YY, Ultrafiltration hollow fiber membranes of sulfonated polyetherimide/polyetherimide blends: preparation, morphologies and anti-fouling properties, *J Membr Sci*, **218**, 279-293, 2003.

19. Qin JJ, Chung TS, Effect of dope flow rate on the morphology, separation performance, thermal and mechanical properties of ultrafiltration hollow fibre membranes, *J Membr Sci*, **157**, 35-51, 1999.

20. Buonomenna MG, Macchi P, Davoli M, Drioli E, Poly(vinylidene fluoride) membranes by phase inversion: the role the casting and coagulation conditions play in their morphology, crystalline structure and properties, *Eur Polym J*, **43**, 1557-

www.SID.ir

1572, 2007.

21. Lin DJ, Beltsis K, Chang CL, Chen LP, Fine structure and formation mechanism of particulate phase-inversion poly(vinylidene fluoride) membranes, *J Polym Sci, Part B: Polym Phys*, **41**, 1578-1588, 2003.

22. Deshmukh SP, Li K, Effect of ethanol composition in water coagulation bath on morphology of PVDF hollow fibre membranes, *J Membr Sci*, **150**, 75-85, 1998.

23. Xu AT, Yang AH, Young S, De Montigny D, Tontiwachwuthikul P, Effect of internal coagulant on effectiveness of polyvinylidene fluoride membrane for carbon dioxide separation and absorption, *J Membr Sci*, **311**, 153-158, 2008.

24. Song MK, Kim YT, Fenton JM, Kunz HR, Rhee HW, Characteristics of PVDF copolymer/Nafion blend membrane for direct methanol fuel cell (DMFC), *J Power Sources*, **50**, 583-588, 2004.

25. Cho KY, Eom JY, Jung HY, Choi NS, Lee YM, Park JK, Choi JH, Park KW, Sung YE, Characteristics of PVDF copolymer/Nafion blend membrane for direct methanol fuel cell (DMFC), *Electrochim Acta*, **50**, 583-588, 2004.

26. Song MK, Kim YT, Fenton JM, Kunz HR, Rhee HW, Chemically-modified Nafion/poly(vinylidene fluoride) blend ionomers for proton exchange membrane fuel cells, *J Power Sources*, **117**, 14-21, 2003.

27. Lang WZ, Xu ZL, Yang H, Tong W, Preparation and characterization of PVDF-PFSA blend hollow fiber UF membrane, *J Membr Sci*, **288**, 123-131, 2007.

28. Mulder M, *Basic Principle of Membrane Technology*, 2nd ed, Kluwer Academic, Boston, 1996.

29. Li JF, Xu ZL, Yang H, Feng CP, Shi JH, Hydrophilic microporous PES membranes prepared by PES/PEG/DMAc casting solutions, *J Appl Polym Sci*, **107**, 4100-4108, 2008.

30. Khayet M, Feng CY, Khulbe KC, Matsuura T, Study on the effect of a non-solvent additive on the morphology and performance of ultrafiltration hollow-fiber membranes, *Desalination*, **148**, 321-327, 2002.

31. Brandrup J, Immergut EH, Grulke EA, *Solubility Parameter Values,* In: *Polymer Handbook*, Wiley,

New Work, 1999.

32. Wang YJ, Kim D, The effect of F127 addition on the properties of PEGDA/PVDF cross-linked gel polymer electrolytes, *J Membr Sci*, **312**, 76-83, 2008.

33. Reuvers AJ, Van BJ, Smolders CA, Formation of membranes by means of immersion precipitation: Part I. A model to describe mass transfer during immersion precipitation, *J Membr Sci*, **34**, 45-65, 1987.

34. Reuvers AJ, Smolders CA, Formation of membranes by means of immersion precipitation: Part II. The mechanism of formation of membranes prepared from the system cellulose acetate-acetone-water, *J Membr Sci*, **34**, 67-86, 1987.

35. Yang XT, Xu ZL, Wei MY, Effect of additives on the demixing rate and membrane performance of PVDF membrane, *Membr Sci Tech China*, **27**, 26-30, 2007.

36. Bottino A, Camera-Roda G, Capannelli G, Munari S, The formation of microporous polyvinylidene difluoride membranes by phase separation, *J Membr Sci*, **57**, 1-20, 1991.

37. Paddison SJ, Elliott JA, On the consequences of side chain flexibility and backbone conformation on hydration and proton dissociation in perfluorosulfonic acid membranes, *Phys Chem Chem Phys*, **8**, 2193-2203, 2006.

38. Young TH, Cheng LP, Lin DJ, Fane L, Chuang WY, Mechanisms of PVDF membrane formation by immersion-precipitation in soft (1-octanol) and harsh (water) nonsolvents, *Polymer*, **40**, 5315-5323, 1999.

39. Marchese J, Ponce M, Ochoa NA, Pradanos P, Palacio L, Hernandez A, Fouling behaviour of polyethersulfone UF membranes made with different PVP, *J Membr Sci*, **211**, 1-11, 2003.

40. Cheng LP, Lin DJ, Shih CH, Dwan AH, Gryte CC, PVDF membrane formation by diffusion-induced phase separation-morphology prediction based on phase behavior and mass transfer modeling, *J Polym Sci, Part B: Polym Phys*, **37**, 2079-2092, 1999.